SERENDIPITOUS INORGANIC HELIX FORMATION FROM A pH RESPONSIVE INORGANIC COMPLEX

by

Emily C. Hoffer

Submitted in partial fulfillment of the

requirements for Departmental Honors in

the Department of Chemistry and Biochemistry

Texas Christian University

Fort Worth, Texas

May 3, 2021

SERENDIPITOUS INORGANIC HELIX FORMATION FROM A PH SENSITIVE

INORGANIC COMPLEX

Project Approved:

Supervising Professor: Kayla N. Green, Ph.D.

Department of Chemistry & Biochemistry

Julie Fry, Ph.D.

Department of Chemistry & Biochemistry

Mikaela Stewart, Ph.D.

Department of Biology

ABSTRACT

The Green research group has developed a library of tetraaza macrocyclic ligands with the potential to treat neurodegenerative diseases by binding free metals, scavenging radicals, and reducing oxidative stress. The copper complex of one of these ligands, **^{OH}PyN$_3$Cu**, was discovered to form a novel helix structure upon crystallization around pH 6.5. To understand the mechanism and driving forces that led to formation of this helix, we investigated several aspects of the ligand. Density-functional Theory (DFT) studies, a comparison of keto/enol tautomerization stability, and a comparison of bond lengths, were considered to determine the protonation state of the pyridol moiety and, therefore, the character of the bond between the subunits of the helix. We also considered other structural aspects of **Cu1$_H$** including the interactions with perchlorate counterions and the symmetry of **Cu1$_H$**. Because **Cu1$_H$** does not exhibit the typical factors that stabilize the formation of helices, such as intrastrand hydrogen bonding or pi stacking, we conclude that perchlorate templating through hydrogen bonding between perchlorate counterions and **Cu1$_H$** is the primary driving factor of helix formation. The discovery of this helix structure further highlights the diversity of inorganic metallohelices and demonstrates the importance of tautomerization and pH, as well as counterions in designing drugs and other molecules.

ACKNOWLEDGEMENTS

I would like to thank everyone who made this project possible, including my committee, the TCU John V. Roach Honors College, the TCU College of Science and Engineering, and the TCU Department of Chemistry and Biochemistry.

First, my sincerest gratitude to Dr. Green. Thank you for your endless patience and confidence in my abilities. From semesters when I didn't have much time to dedicate to research to helping me switch projects for my thesis to pushing me to learn new things, you've constantly been supportive, patient, there to guide me. I want to thank you for being a role model and helping shape me into the scientist I have become.

I also want to thank both current and former members of the Green Group. I am so lucky to be part of a group that I can always count on for support and friendship. You all have taught me so much and I could not have succeeded without you. To Nam, Nishu, and Diandria, thank you for your camaraderie, humor, and dedication. I've learned a lot from you and will truly miss the "Green Beans." To Maddie Barnett, thank you for being a chemistry student, and now a medical student, I can look up to. I turned to your old presentations and papers many times for guidance, and I am so grateful for your help and support as I applied to medical school. Brian, this project would literally not exist without you. I am so grateful for your discovery several years ago that led me to this project and want to thank you for working with me on my very first project as a member of the Green Group. Kristof, you have been so incredibly helpful throughout my time in the Green Research group, including the work on my honors thesis. I am published because of you and I have learned so much from you. David, I am sorry our initial project did not work out. I thoroughly enjoyed working with you on the biosensors (and am especially grateful

for that time you came back to help when I broke the centrifuge). You helped me so much through that project and were a huge part of my experience in the Green Group. To everyone else, thank you so much for your time and encouragement. I could always count on your kindness and help, and it was y'all who made my experiences in Green Group so amazing.

Additionally, my sincerest thanks to Timothy Prior and his assistance with our XRD analysis, but most importantly for drawing our attention to the importance of the perchlorate ions.

TABLE OF CONTENTS

LIST OF FIGURES

LIST OF TABLES

INTRODUCTION

I. Metallohelices

Helices are three-dimensional structures that often result from inter- and intramolecular forces within a molecule or molecules. These unique assemblies serve as critical components for many biological structures; the best-known examples include the double helix of DNA and the many derivatives of alpha helices in protein backbones. Aside from the biological importance of helices, metallohelices have been widely reported in the literature and serve a variety of purposes.[1-5] Gieck and coworkers reported an interlocking screw helix composed of uranium orthothiophosphates.[1] A thymidine chiral helix structure was designed by Roth and coworkers to enhance enantioselective recognition processes (Figure 1a).[2] Dey and coworkers reported a helix composed of a copper(II) complex with syn- and anti-carboxylate bridges (Figure 1b).[3] Moreover, Lehn and coworkers reported that oligobipyridine ligands and copper(I) spontaneously formed a double-stranded helicate with the copper(I) cations at the center of the structure, which offered the opportunity for further study of systems involving self-organization, cooperativity, and chirality within a helix, applications to organic and inorganic chemistry, as well as the potential ability to bind and cleave DNA with specialized selectivity.[4] Some metallohelices have proven biological applications. For example, the solid-state structure of the antiarthritic drug gold thiomalate was reported to form a double helix (Figure 1c).[5]

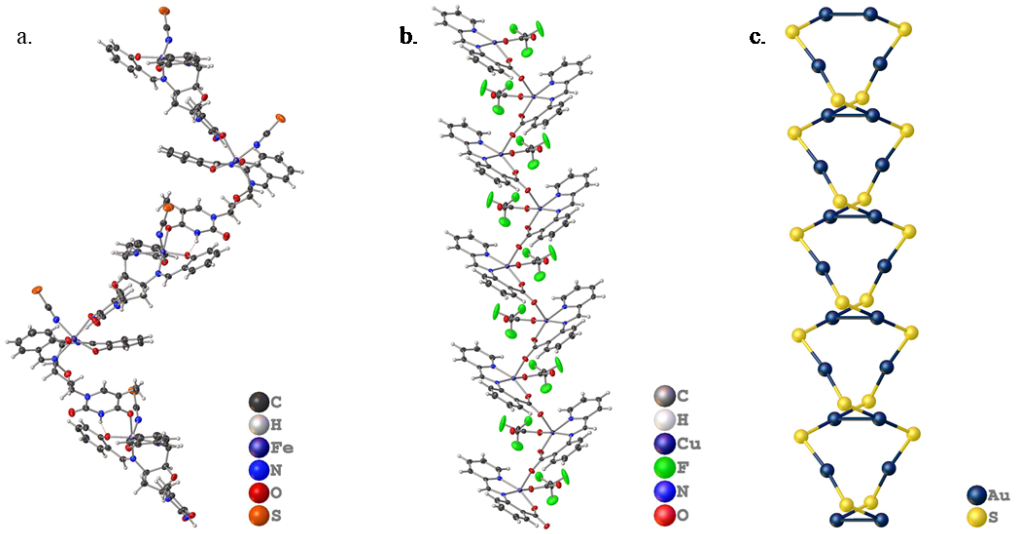

Figure 1. Representative examples of metallohelices reported to date. a) Thymidine chiral helix,[2] b) Copper (II) complex with syn- and anti-carboxylate bridges helix,[3] c) Thiomalate double helix with the helix Au-S core shown.[5]

II. Tetraaza Macrocyclic Ligands and an $^{OH}PyN_3$ Helix

We have reported a library of tetraaza macrocyclic ligands with the potential to target the oxidative stress associated with the development of neurodegenerative diseases such as Alzheimer's. The copper(II) complex of the tetraaza pyridinophane **$^{OH}PyN_3$** (**1**, Figure 2a), has been shown to have enhanced antioxidant capabilities compared to parent macrocyclic structures and provided positive results with biological and pharmacological studies, suggesting it could have therapeutic effects against neurodegenerative diseases.[6-9] In our original report, we observed a mononuclear, pentacoordinate copper complex (**Cu1$_M$**, Figure 2b).[8] As a result of a recent revisitation to this work and using a modified procedure, copper(II) complexes of **1** were observed to form crystals with a helix structure (**Cu1$_H$**) at around pH 6.5 (Figure 2c-e). Here we present the X-ray diffraction study of this unique helical structure (**Cu1$_H$**) and relate the results to

potentiometric studies to show that the formation of the helix is correlated to the keto-enol tautomerization of the ligand.

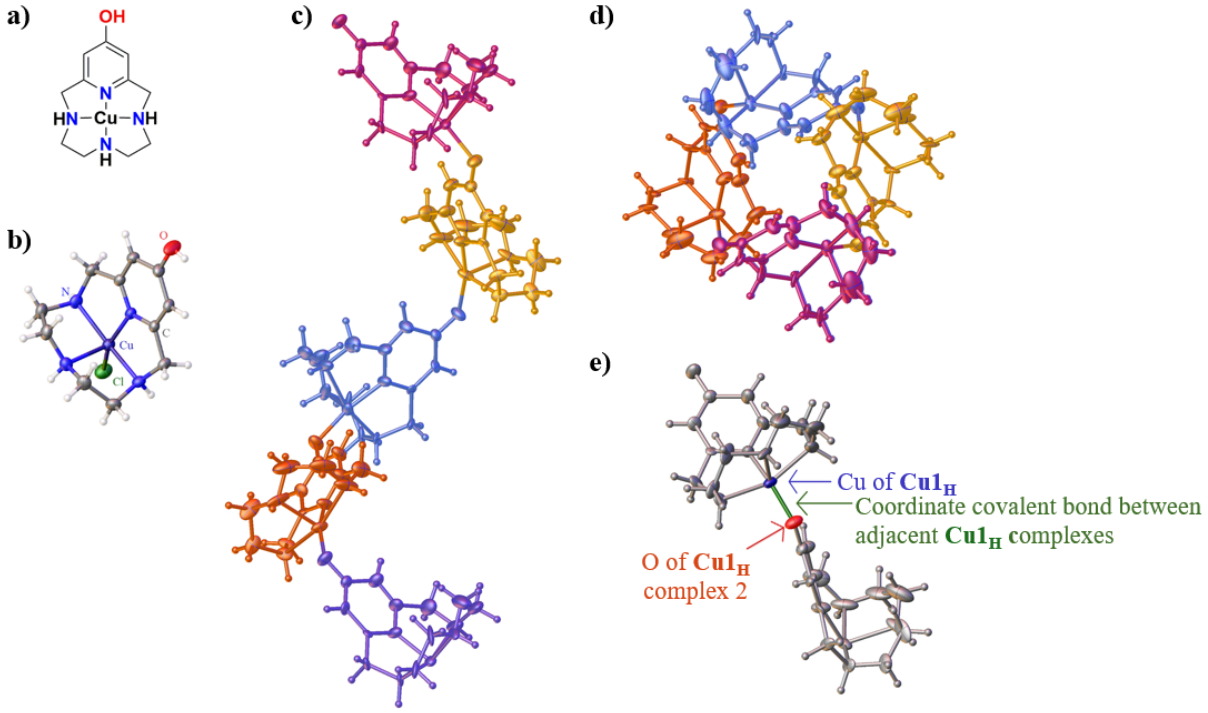

Figure 2. a) Drawing of **Cu1**. b) Solid State structure previously reported[10] for $\mathbf{Cu1_M}$ c) View of the $\mathbf{Cu1_H}$ helix from the side, depicting five $\mathbf{Cu1_H}$ units. d) View of $\mathbf{Cu1_H}$ helix from the top, which highlights that each rotation is composed of four $\mathbf{Cu1_H}$ units, evidenced by the complete overlap of the first $\mathbf{Cu1_H}$ unit (pink) with the fifth $\mathbf{Cu1_H}$ unit (violet) e) A coordinate covalent bond between the Cu of one $\mathbf{^{OH}PyN_3Cu}$ complex and the O-atom of an adjacent $\mathbf{^{OH}PyN_3Cu}$ complex connects $\mathbf{^{OH}PyN_3Cu}$ units to form the helix structure.

RESULTS AND DISCUSSION

I. Overview of the $Cu1_H$ Crystal Structure

We have previously reported that monomeric copper(II) complexes of **Cu1** are obtained by the addition of copper(II) perchlorate to a solution of ligand **1** in water at pH 7.[8, 10] Using this method, the pH of the solution drops to 2-3 after stirring overnight, but the copper(II) complex

(Figure 2a-b) forms in good yields. X-ray diffraction analysis of single crystals obtained by slow evaporation showed discrete monomeric **Cu1$_M$** complexes. Each copper(II) ion was bound to the four N-atoms of the pyridinophane macrocycle with a chloride ion as a fifth coordinating ligand. The hydroxyl group on the 4-position of the pyridine ring displayed a hydrogen bond to the adjacent perchlorate counter ion, but no interactions were observed between **Cu1$_M$** units. However, a markedly different solid-state structure was observed when this procedure was repeated but with continued adjustment of the pH to roughly 6.5. Blue single crystals were obtained by slow evaporation of the aqueous mother liquor. Analysis using X-ray diffraction at 100 K resulted in the model shown in Figure 2c-e. The helical nature of the **Cu1$_H$** structure is evident when viewed from the top-down. Four **Cu1** units are required to complete one full rotation of this right-handed helix, which is composed of a **Cu1** consecutively connected through a coordinate covalent bond between the O-atom of the ligand **1** with the copper(II) ion of the adjacent **Cu1$_H$** complex (Figure 2e). Perchlorate anions are disordered throughout, which complicates the structural analysis. Each perchlorate occupies two different orientations in equal amounts and this is a consequence of the high symmetry space group; each chloride resides on a 4*a* Wyckoff position with site symmetry (..2). There are N-H…O interactions observed between the helices and the perchlorate counterions, which reside in the groove formed from turns in the helix. A packing diagram reveals that the groove of one helix unit interlocks with the curve of an adjacent helix (Figure 3b-c).

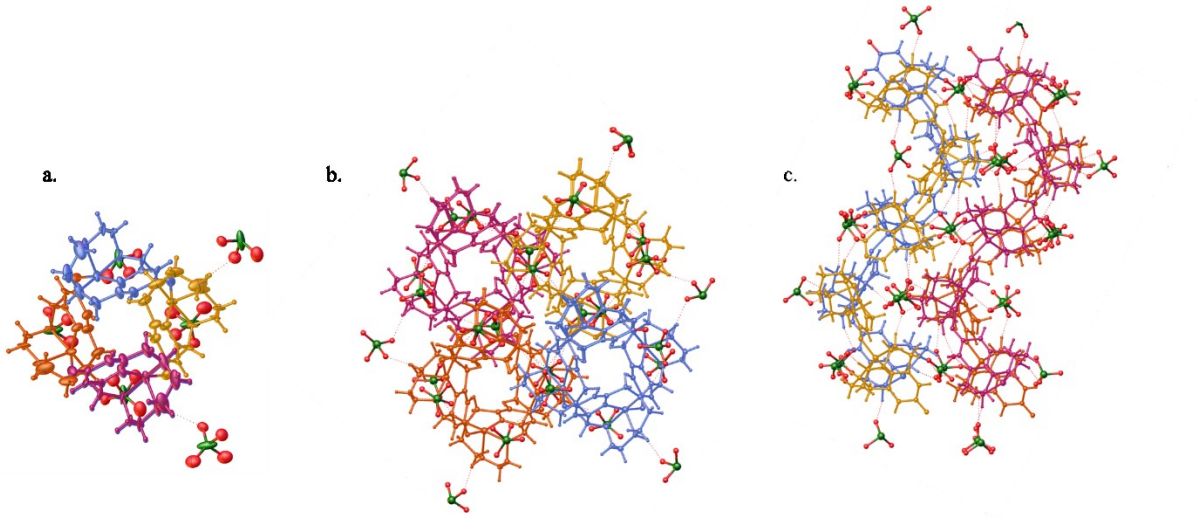

Figure 3. a) A top-down view of a single strand of the **Cu1$_H$** with perchlorate counterions b) A top-down view of four strands of **Cu1$_H$** packed, including perchlorate counterions. c) A side view of four strand of **Cu1$_H$** packed, including perchlorate counterions.

II. Tautomer Determination

We hypothesized that the pH of the solution during complexation and crystallization was responsible for the modulated speciation of the **Cu1** complex between the mononuclear complex observed previously and this newly observed helix. This is supported by several observations. Ligand **1** undergoes a keto-enol tautomerization, favoring the keto form between pH values of 5.45 – 9.0.[6] Likewise, the **Cu1** complex also undergoes a protonation event in a similar pH range (Scheme 1, Figure 4). For comparison, while the enol tautomer was observed to be more stable than the keto form of the dianionic form of chelidamic acid (**2^{2-}**), the keto tautomer was preferred with the **2Me$_2$** congener (Figure 5).[11, 12] The shift in preference for enol vs. keto is due to the

methyl ester being more electron-withdrawing than the deprotonated carboxyl. Therefore, it is reasonable to consider that the copper(II) cation of **Cu1** has an electron-withdrawing effect on the pyridol ring, which would similarly stabilize the keto form of the complex. The deprotonation of the **Cu1** complex creates the opportunity for the interchelate bond to form, and the strand becomes the thermodynamically favored structure over the monomeric unit.

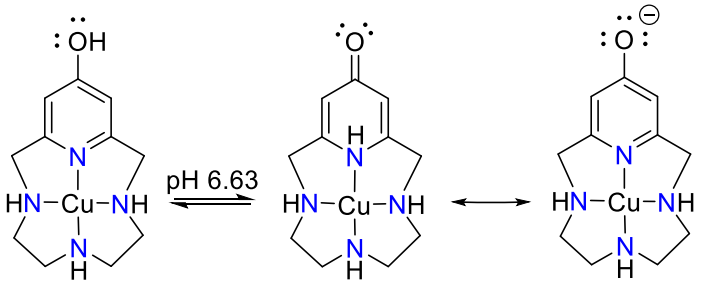

Scheme 1. Keto-enol tautomerization of **Cu1**$_M$.[6]

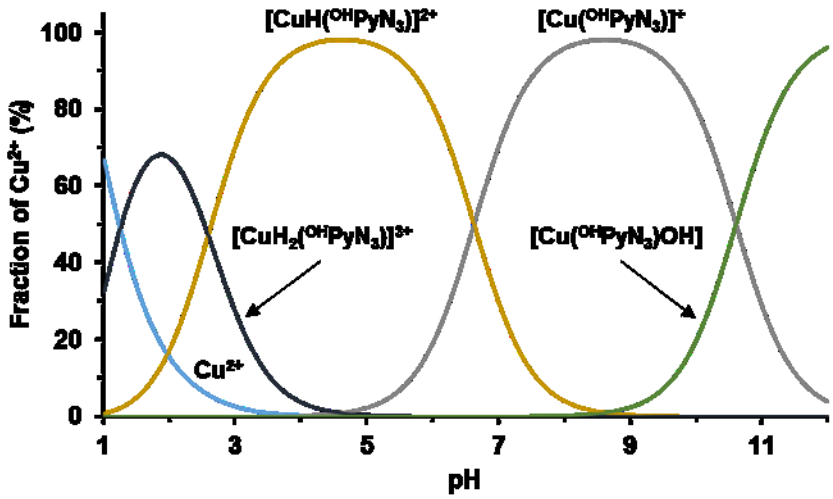

Figure 4. Equilibrium distribution diagram of the **Cu(II)-^{OH}PyN$_3$** system.[6]

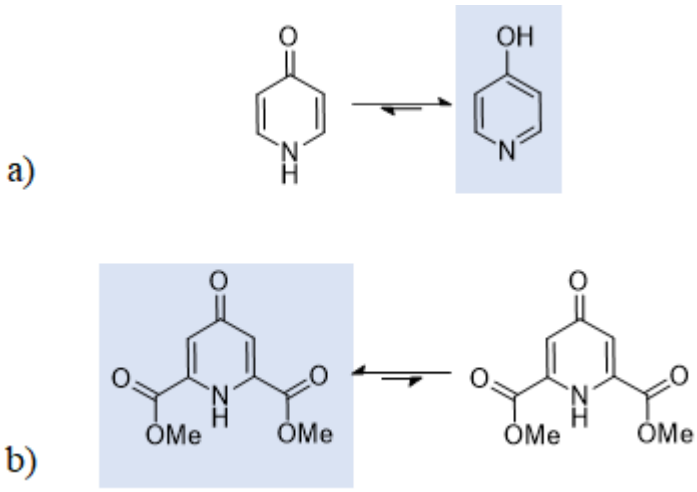

Figure 5. a) The enol tautomer of chelidamic acid [2^{2-}] is more stable than the keto tautomer. b) When electron-withdrawing methyl ester groups replace the carboxylate groups [**2Me$_2$**], the keto tautomer is more stable than the enol tautomer.

Furthermore, inspection of the bond lengths within the solid-state structure of **Cu1$_H$** support that the keto tautomer is prevalent. The C-O bond length (1.278 Å) lies more closely to the keto form of [**2Me$_2$**] (1.274 Å) compared to the enol form of [**2^{2-}**] (1.331 Å) and monomeric **Cu1$_M$** (1.340 Å) (Figure 6).[10, 13-15]

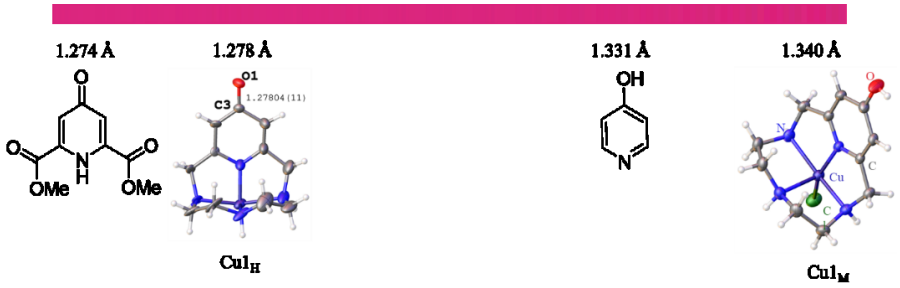

Figure 6. Comparison of C-O bond lengths reveals that the C-O bond length in **Cu1$_H$** is close to the C-O bond length in the keto form of **2Me$_2$**.

Additionally, DFT analysis was used to determine whether the keto or enol tautomer was preferred in the solid state. **Cu1$_H$** was modeled with a coordinated aqua ligand, using wB97XD[16] with the 6-31+g(d,p)[17] basis set and a water SMD[18] solvent model. First, the relaxed geometry was determined, followed by fixing the C-O bond length to specific lengths. The fixed bond lengths chosen were 1.2736 Å, 1.298 Å, and 1.349 Å. These correspond to the bond lengths found in the crystal structures of 4-pyridone[19, 20], **Cu1$_H$**, and 4-nitrophenol[21], respectively. The 4-pyridone bond length was chosen as the model for the keto form because it exhibits a preference for the keto tautomer. The 4-nitrophenol bond length was chosen as the model for the enol form because the electronics of pyridine are more akin to nitrobenzene. Therefore, the 4-nitrophenol bond length is more applicable than phenol itself. Each model had no imaginary frequencies.

As shown in Figure 7, the energy values of each fixed bond length were compared to the relaxed geometry, which was found to have a bond length of 1.27997 Å. The enol congener had a much higher energy of 9.903386 kJ/mol, while the keto congener had an energy of 0.572359 kJ/mol, both relative to the relaxed geometry. The solid-state bond length in **Cu1$_H$** is much closer to both the relaxed and keto geometries, with an energy of 0.627494 kJ/mol, relative to the relaxed geometry. Ultimately, it was deduced that **Cu1$_H$** exists as the keto tautomer. We propose then that the bond order between the carbon-oxygen atoms is closer to two, containing both sigma and pi electrons.

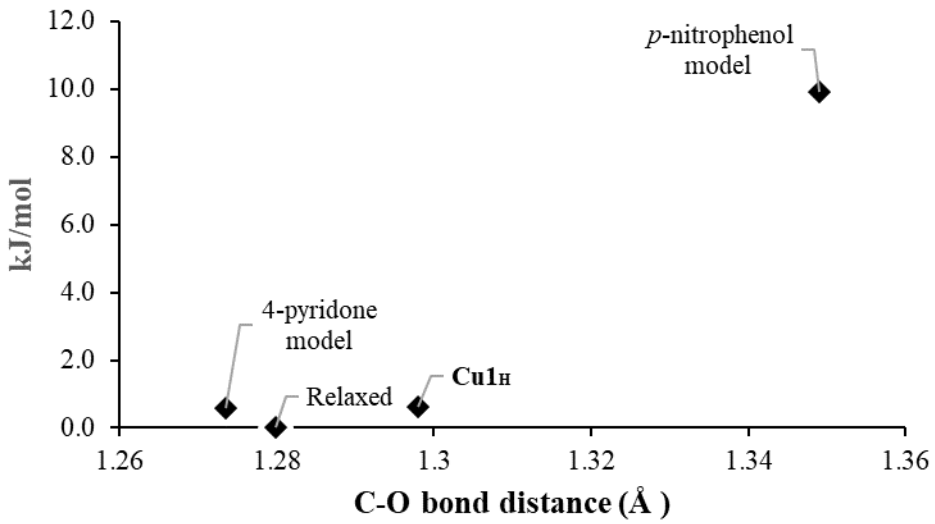

Figure 7. Energy values of **Cu1$_H$** with fixed bond lengths, corresponding to the bond length of 4-pyridone[19, 20], the solid-state structure of **Cu1$_H$**, and the bond length of *p*-nitrophenol[21], all relative to the relaxed geometry.

III. Perchlorate Templating

Having established that the **Cu1···O** interaction was facilitated by the keto form of the **^{OH}PyN$_3$Cu** complex, we set out to determine what properties further facilitated the helical structure observed in the solid state. When comparing our structure to many other helix structures, we do not find many of the common interactions that typically lead to helix formation. For example, an alpha helix in a peptide is held together by hydrogen bonding between amide functional groups in the backbone. Similarly, hydrogen bonding between the purine and pyrimidine bases of two strands of the double helix and pi stacking are attributed to the double helix of DNA. The **Cu1$_H$** helix is single-stranded and, therefore, cannot be stabilized by hydrogen bonding between two strands as is observed in structure like DNA. Furthermore, no evidence of hydrogen bonding within **Cu1$_H$** is observed, which would stabilize the conformation, and there is no evidence of aromatic stacking between the pyridine rings within one helix or between

adjacent helices. The closest contacts are between the H-atom on N4 and H4 of the adjacent **Cu1$_H$** unit. One previous example of a metallohelix reported by Lehn and coworkers was stabilized by the presence of cations at the center of the helix.[4] Although our helix contains the copper(II) cation, these cations are located within the strand and do not provide a framework for our ligand to surround.

Although the copper(II) cations cannot provide a framework for the helix, we propose that the presence of the perchlorate anions is the driving force for the formation of the helical structure through the hydrogen bonds they create with the strands of connected complexes. The ability of perchlorate ions to template or stabilize the formation of helical three-dimensional structures from polymers such as peptides has been reported in the literature.[22] However, to our knowledge perchlorate templating has not yet been reported to facilitate helix formation in structures such as **^{OH}PyN$_3$Cu** or other macrocycles that typically exist as monomers. Each perchlorate ion is found in a "pocket" of the helix and forms N-H…O hydrogen bonds to adjacent strands of **Cu1$_H$** (Figure 8). A slight asymmetry of each **Cu1$_H$** unit is observed, which is observed with the **Cu1$_M$** that contained a mirror plane from the hydroxyl moiety through the copper(II) ion. The degree of the twist is evident with the positions of the C-atoms alpha to the pyridine ring. This can be estimated by comparing the twist in the planes formed between C1C2C3N1 (177°) and C2C3C4N1 (174°) as shown in Figure 9. The side of the molecule with the larger angle is located in the interior of the helix rotation and the N-atom forms a H-bond with one of the perchlorate ions in the helix groove. Conversely, the opposite plane is located on the exterior side of the helix with no H-bonds observed (Figure 9). We propose that the presence of hydrogen bonding to the perchlorate ions creates this asymmetry, slightly pulling the interior side of **Cu1$_H$**

toward the perchlorate ion and thereby creating the rotation necessary for a strand of **Cu1$_H$** to twist into the helix conformation.

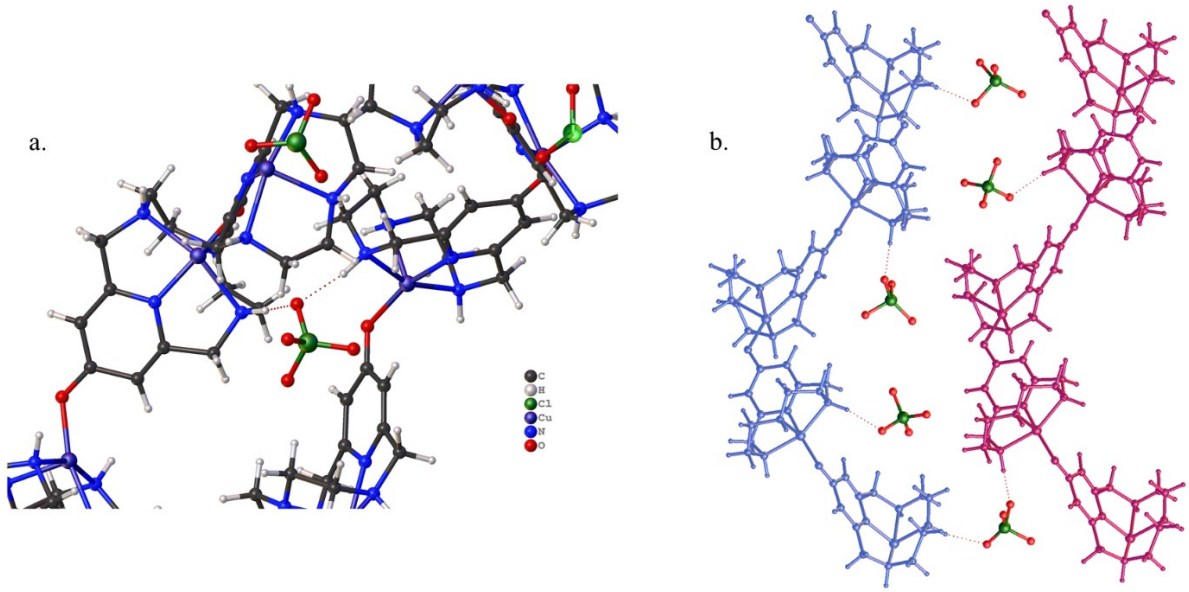

Figure 8. a) N-H…O hydrogen bonding occurs between an oxygen atom of perchlorate and a hydrogen atom of **Cu1$_H$**. b) Perchlorate ions between two strands of **Cu1$_H$**. The ions are found along the interior curve of the helix.

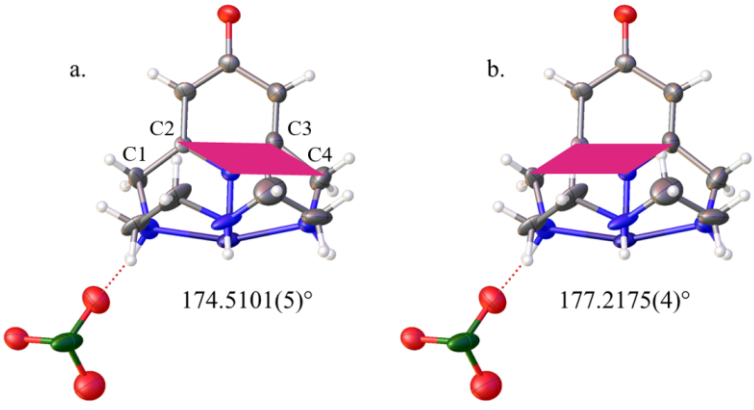

Figure 9. a) The degree of rotation on the exterior side of **Cu1$_H$** is 174.5101(5)°. b) The degree of rotation on the interior side of **Cu1$_H$**, which is hydrogen bonded to a perchlorate ion, is larger at 177.2175(4)°.

IV. Temperature Dependence

To study the behavior of $Cu1_H$, we measured distances and angles within the helix at a range of temperatures during diffraction. Small differences were observed in the turn of the helix, length and width of the helix, bond distances, and packing widths (see Appendix for data). However, these differences are not atypical of what is expected over a range of temperatures with complexes of this type.

METHODS

I. General Methods

Methanol was distilled from KOH and stored over 4 Å molecular sieves. Other solvents and chemicals were purchased from commercial sources and used as received. A Leica MZ 75 microscope was used to identify samples suitable for analysis. A Bruker APEX-II CCD diffractometer was employed for crystal screening, unit cell determination, and data collection, which were obtained at 100 K. The Bruker D8 goniometer was controlled using the APEX3 software suite.[23] The samples were optically centered with the aid of a video camera so that no translations were observed as the crystal was rotated through all positions. The X-ray radiation employed was generated from a Mo Kα sealed X-ray tube (λ = 0.71076 Å) with a potential of 50 kV and a current of 30 mA, fitted with a graphite monochromator in the parallel mode (175 mm collimator with 0.5 mm pinholes).

Synthesis of $Cu1_H$. Ligand **1** was prepared according to literature.[10] The copper complex was prepared in accordance with the same report but with monitoring the pH using a pH probe. The pH was adjusted to 6.5-7. The reaction was considered complete when the pH no longer changed.

II. X-ray Diffraction Analysis

Cu1$_H$ crystallized as aggregates of blocks from an aqueous solution. All of the crystals examined were found to be multiple crystals. The crystal examined showed the presence of a single dominant domain, but the diffraction data were still contaminated by the presence of at least one other domain. The nature of the overlap of spots from the two principal domains precluded de-twinning of the data and it was not possible to carry out multi-domain integration of the data. We hope to return to this problem in the future after further recrystallizations from a wide variety of different solvents. The data from the principal domain are of acceptable quality (R factor (R_{int}) = 0.1391) and we have used these to solve the structure. Initially the structure was solved by dual-space methods in the orthorhombic space group $P2_12_12_1$. However, PLATON revealed additional symmetry was present and the structure was transformed to $P4_32_12$. Satisfactory refinement of the structure as a racemic twin (Flack parameter 0.139(13) (Parson's method) was possible and this yielded a straightforward determination of the structure that confirmed the atomic connectivity. Due to the nature of the crystal examined the quality of fit parameters are not particularly good but this does not change the soundness of the determination of the atomic arrangement.

CONCLUSION

Using X-ray diffraction, we discovered that **^{OH}PyN$_3$Cu** complex forms a single-stranded helix when crystallized at a pH around 6.5. We have shown that the solution pH plays an important role in the speciation of the **Cu1$_H$** complex and the subsequent formation of a coordinate covalent bond between the copper(II) ion of one **^{OH}PyN$_3$Cu** complex and the O-atom of an adjacent **^{OH}PyN$_3$Cu**

complex. Based on potentiometric data, a deprotonation event occurs at around pH 6.63. Comparison to chelidamic acid studies, bond lengths, DFT analysis, and previous studies of protonation constants of the ligand support that the complex favors the keto congener at this pH. Hydrogen bonding or π-stacking were not observed within the helix. Hydrogen bonding between perchlorate counterions and **$Cu1_H$**, however, was observed, along with a slight asymmetry of each **$Cu1_H$** complex. Therefore, we conclude that the perchlorate ions are templating the formation of the three-dimensional solid-state helix structure as a result of the asymmetry of **$Cu1_H$**-induced by hydrogen bonding to perchlorate ions.

APPENDIX

I. X-ray Diffraction Tables

Table 1. Crystal data and structure refinement for $Cu1_H$

Identification Code	Tet	
Empirical Formula	$C_{44}H_{68}Cl_4Cu_4N_{16}O_{20}$	
Formula Weight	1537.119	
Temperature	100.15 K	
Crystal system	tetragonal	
Space group	$P4_32_12$	
Unit Cell dimensions	a = 11.5720(17) Å	α = 90°
	b = 11.5720(17) Å	β = 90°
	c = 21.939(3) Å	λ = 90°
Volume	2937.9(8) $Å^3$	
Z	2	
ρ_{calc}	1.738 g/cm	
Absorption coefficient	1.698 mm^{-1}	
F(000)	1580.7	
Crystal size	N/A × N/A × N/A mm^3	
Radiation	Mo Kα (λ = 0.71076)	
2θ range for data collection	6.22° to 50.02°	
Index ranges	-12 ≤ h ≤ 12, -13 ≤ k ≤ 12, -28 ≤ l ≤ 27	
Reflections collected	49399	
Independent reflections	2536 [R_{int} = 0.1400, R_{sigma} = 0.0796]	

Data / restraints / parameters	2536/70/227	
Goodness of fit on F^2	1.180	
Final R indices [I>=2σ (I)]	R_1 = 0.1258, wR_2 = 0.2684	
Final R indices [all data]	R_1 = 0.1446, wR_2 = 0.2787	
Largest diff. peak and hole	1.31/-1.54 e $Å^{-3}$	
Flack parameter	0.21(8)	

Table 2. Bond lengths (Å) for $Cu1_H$

Atom	Atom	Length		Atom	Atom	Length
C1	C2	1.38(2)		C11	O4	1.416(13)
C1	C6	1.47(2)		C12	$O5^2$	1.369(12)
C1	N1	1.418(19)		C12	O5	1.369(12)
C2	C3	1.35(2)		C12	O6	1.408(13)
C3	C4	1.46(2)		C12	$O6^2$	1.408(13)
C3	O1	1.281(18)		C12	O7	1.423(13)
C4	C5	1.29(3)		C12	$O7^2$	1.423(13)
C5	C11	1.51(3)		C12	$O8^2$	1.421(12)
C5	N1	1.38(2)		C12	O8	1.421(12)
C6	N2	1.512(19)		Cu1	N1	1.883(15)
C7	C8	1.51(3)		Cu1	N2	2.074(14)
C7	N2	1.44(2)		Cu1	N4	2.132(16)
C8	NA	1.48(3)		Cu1	NA	2.151(19)
C9	C10	1.55(4)		Cu1	$O1^3$	1.917(11)
C9	NA	1.41(3)		O3	$O4^1$	1.09(3)
C10	N4	1.41(4)		O4	$O4^1$	1.70(3)
C11	N4	1.50(3)		O5	$O7^2$	1.24(3)
C11	O2	1.454(12)		O5	$O8^2$	1.59(2)
C11	$O2^1$	1.454(12)		O6	$O6^2$	1.28(4)
C11	$O3^1$	1.513(14)		O6	$O8^2$	1.71(3)
C11	O3	1.513(14)		O7	$O8^2$	1.68(3)
C11	$O4^1$	1.416(13)				

Table 3. Bond angles (°) for $Cu1_H$

Atom	Atom	Atom	Angle		Atom	Atom	Atom	Angle
C6	C1	C2	128.1(14)		$O8^2$	Cl2	$O6^2$	107.3(11)
N1	C1	C2	118.6(14)		$O8^2$	Cl2	O6	74.2(14)
N1	C1	C6	113.1(13)		O8	Cl2	$O6^2$	74.2(14)
C3	C2	C1	124.9(16)		O8	Cl2	O6	107.3(11)
C4	C3	C2	115.0(14)		O8	Cl2	$O7^2$	72.2(14)
O1	C3	C2	122.7(15)		O8	Cl2	O7	106.6(11)
O1	C3	C4	122.0(15)		$O8^2$	Cl2	$O7^2$	106.6(11)
C5	C4	C3	118.8(17)		$O8^2$	Cl2	O7	72.2(14)

C11	C5	C4	125.6(17)	O8	Cl2	$O8^{2}$	178.4(19)
N1	C5	C4	127.6(19)	N2	Cu1	N1	84.4(5)
N1	C5	C11	106.5(17)	N4	Cu1	N1	80.3(7)
N2	C6	C1	112.0(12)	N4	Cu1	N2	158.8(6)
N2	C7	C8	114.9(17)	NA	Cu1	N1	99.0(6)
NA	C8	C7	108.5(16)	NA	Cu1	N2	85.0(6)
NA	C9	C10	106(2)	NA	Cu1	N4	82.9(8)
N4	C10	C9	116(2)	$O1^{3}$	Cu1	N1	162.3(6)
N4	C11	C5	113.9(17)	$O1^{3}$	Cu1	N2	96.3(5)
O2	Cl1	$O2^{1}$	109.1(13)	$O1^{3}$	Cu1	N4	102.7(6)
O3	Cl1	$O2^{1}$	104.8(11)	$O1^{3}$	Cu1	NA	98.7(6)
O3	Cl1	O2	96.7(10)	C5	N1	C1	114.7(15)
$O3^{1}$	Cl1	$O2^{1}$	96.7(10)	Cu1	N1	C1	117.1(11)
$O3^{1}$	Cl1	O2	104.8(11)	Cu1	N1	C5	125.6(13)
$O3^{1}$	Cl1	O3	142.6(18)	C7	N2	C6	111.3(14)
O4	Cl1	O2	102.7(9)	Cu1	N2	C6	107.8(10)
$O4^{1}$	Cl1	O2	135.0(11)	Cu1	N2	C7	105.6(10)
O4	Cl1	$O2^{1}$	135.0(11)	C11	N4	C10	116.8(17)
$O4^{1}$	Cl1	$O2^{1}$	102.7(9)	Cu1	N4	C10	104.8(17)
$O4^{1}$	Cl1	$O3^{1}$	102.1(11)	Cu1	N4	C11	106.1(13)
O4	Cl1	O3	102.1(11)	C9	NA	C8	117.4(19)
O4	Cl1	$O3^{1}$	43.7(13)	Cu1	NA	C8	105.2(11)
$O4^{1}$	Cl1	O3	43.7(13)	Cu1	NA	C9	107.5(19)
O4	Cl1	$O4^{1}$	73.8(15)	$Cu1^{4}$	O1	C3	123.9(12)
O5	Cl2	$O5^{2}$	159.2(17)	$O4^{1}$	O3	Cl1	63.4(12)
$O6^{2}$	Cl2	O5	86.3(14)	$O3^{1}$	O4	$Cl1^{1}$	72.9(12)
O6	Cl2	O5	112.7(11)	$O4^{1}$	O4	$Cl1^{1}$	53.1(8)
O6	Cl2	$O5^{2}$	86.3(14)	$O4^{1}$	O4	$O3^{1}$	107.3(19)
$O6^{2}$	Cl2	$O5^{2}$	112.7(11)	$O7^{2}$	O5	$Cl2^{2}$	66.0(12)
$O6^{2}$	Cl2	O6	53.9(18)	$O8^{2}$	O5	$Cl2^{2}$	56.9(7)
O7	Cl2	$O5^{2}$	52.5(13)	$O8^{2}$	O5	$O7^{2}$	107.1(18)
O7	Cl2	O5	110.6(11)	$O6^{2}$	O6	Cl2	63.1(7)
$O7^{2}$	Cl2	$O5^{2}$	110.6(11)	$O8^{2}$	O6	Cl2	53.3(8)
$O7^{2}$	Cl2	O5	52.5(13)	$O5^{2}$	O7	Cl2	61.5(9)
$O7^{2}$	Cl2	O6	160.7(16)	$O8^{2}$	O7	Cl2	53.8(8)
$O7^{2}$	Cl2	$O6^{2}$	109.1(11)	$O8^{2}$	O7	$O5^{2}$	102.7(14)
O7	Cl2	$O6^{2}$	160.7(16)	$O5^{2}$	O8	$Cl2^{2}$	53.8(7)
O7	Cl2	O6	109.1(11)	$O6^{2}$	O8	$Cl2^{2}$	52.5(9)
$O7^{2}$	Cl2	O7	89(2)	$O6^{2}$	O8	$O5^{2}$	89.0(12)
$O8^{2}$	Cl2	$O5^{2}$	110.3(10)	$O7^{2}$	O8	$Cl2^{2}$	54.0(9)
$O8^{2}$	Cl2	O5	69.4(9)	$O7^{2}$	O8	$O5^{2}$	89.4(14)

O8	Cl2	O5	110.3(10)		$O7^2$	O8	$O6^2$	86.0(11)
O8	Cl2	$O5^2$	69.4(9)					

II. Temperature Data

Table 4. Effect of Temperature on Helix Dimensions

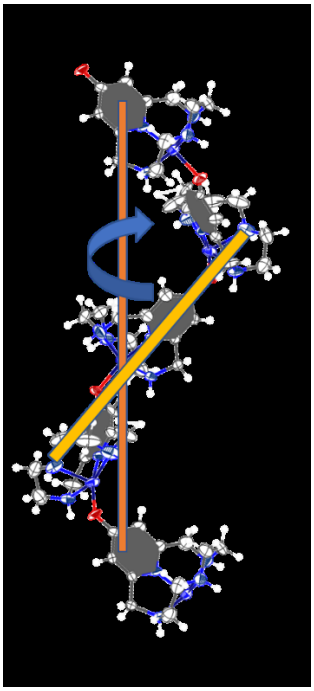

	Temp. (K)	Direction of helix	Turn of helix centroid-centroid	Length of helix centroid-centroid[1]	Width of helix 1(N2)-3(N2)
285K to 105K	285	Left	80.251/99.749	22.006	15.307
	265	Left	80.193/ 99.807	21.977	15.298
	245	Left	80.255/ 99.745	21.990	15.349
	225	Left	80.283/ 99.717	21.993	15.309
	205	Left	80.135/ 99.865	21.984	15.303
	185	Left	80.273/ 99.727	21.989	15.306
	165	Left	80.680/ 99.320	21.996	15.263
	145	Left	80.776/ 99.224	21.999	15.255
	125	Left	81.053/ 98.947	22.009	15.350
105K to 285K	185	Left	80.504/ 99.496	21.979	15.330
	205	Left	80.198/ 99.802	21.980	15.304
	225	Left	80.185/ 99.815	21.971	15.314
	245	Left	80.098/ 99.092	21.988	15.310
	265	Left	80.077/ 99.923	21.990	15.384
	285	Left	80.340/ 99.660	22.006	15.332

Table 5. Effect of Temperature on Bond Dimensions

	Temp. (K)	Bond angle C2-O1-Cu	Bond length C2-O	Bond Length O1-Cu
285K to 105K	285	122.586	1.300	1.923
	265	122.910	1.282	1.915
	245	123.068	1.297	1.916
	225	122.587	1.293	1.922
	205	122.649	1.298	1.922
	185	123.120	1.280	1.917
	165	123.679	1.274	1.912
	145	125.016	1.268	1.938
	125	124.995	1.275	1.928
105K to 285K	185	123.638	1.289	1.980
	205	123.127	1.299	1.919
	225	122.809	1.292	1.925
	245	122.512	1.299	1.923
	265	122.755	1.303	1.937
	285	122.737	1.299	1.932

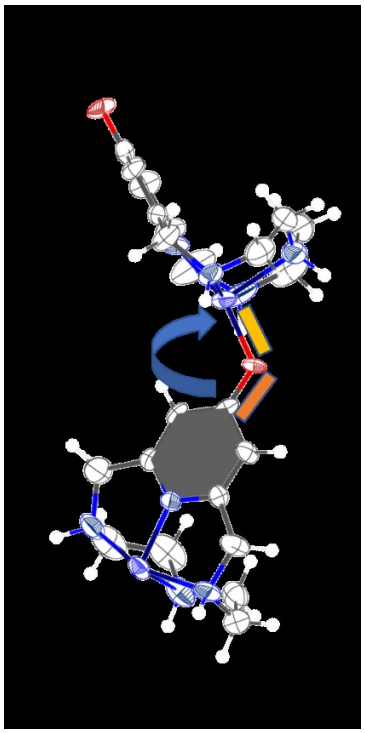

Table 6. Effect of Temperature on Packing Dimensions

	Temp. (K)	Pack width O1-O1	Pack width O2-O2	H bonding Distance
285K to 105K	285	7.421	9.418	1.76
	265	7.407	9.393	1.74
	245	7.402	9.394	1.74
	225	7.392	9.384	1.72
	205	7.371	9.376	1.72
	185	7.365	9.362	1.70
	165	7.365	9.332	1.68
	145	7.365	9.274	2.30
	125	7.372	9.236	2.30
105K to 285K	185	7.378	9.350	2.36
	205	7.386	9.376	1.72
	225	7.391	9.382	1.72
	245	7.400	9.409	1.76
	265	7.495	9.497	1.86
	285	7.433	9.427	1.80

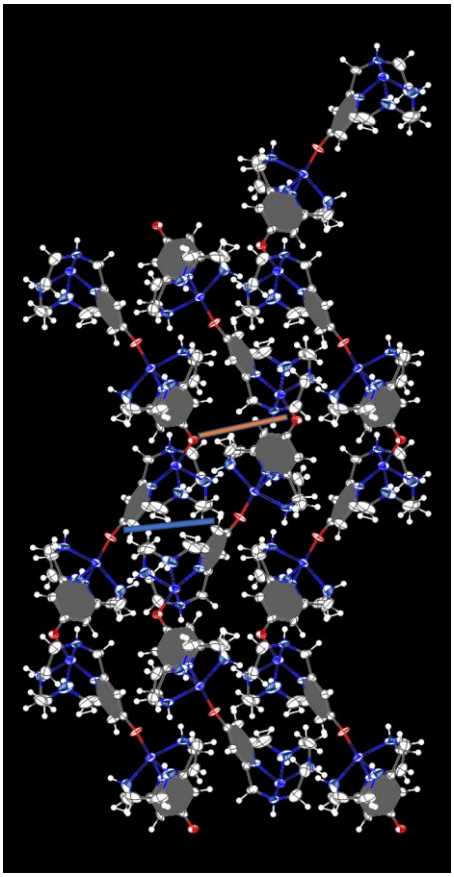

REFERENCES

1. Gieck, C.; Tremel, W., Interlocking Inorganic Screw Helices: Synthesis, Structure, and Magnetism of theNovelFrameworkUraniumOrthothiophoshatesA11U7(PS4)13 (AK,Rb) *Chem. Eur. J.* **2002,** *8* (13).

2. Roth, A.; Koth, D.; Gottschaldt, M.; Plass, W., An Inorganic Thymidine Helix: Design of Homochiral Helical Arrays. *Crystal Growth & Design* **2006,** *6* (12), 2655-2657.

3. Dey, S. K.; Bag, B.; Abdul Malik, K. M.; El Fallah, M. S.; Ribas, J.; Mitra, S., A Quasi-Tetrahedral Cu4Cluster and a Helical-Chain Copper(II) Complex with Single Syn−Anti Carboxylate Bridges: Crystal Structure and Magnetic Properties. *Inorganic Chemistry* **2003,** *42* (13), 4029-4035.

4. Lehn, J. M.; Rigault, A.; Siegel, J.; Harrowfield, J.; Chevrier, B.; Moras, D., Spontaneous assembly of double-stranded helicates from oligobipyridine ligands and copper(I) cations: structure of an inorganic double helix. *Proceedings of the National Academy of Sciences* **1987,** *84* (9), 2565-2569.

5. Bau, R., Crystal Structure of the Antiarthritic Drug Gold Thiomalate (Myochrysine): A Double-Helical Geometry in the Solid State. *Journal of the American Chemical Society* **1998,** *120* (36), 9380-9381.

6. Green, K. N.; Pota, K.; Tircsó, G.; Gogolák, R. A.; Kinsinger, O.; Davda, C.; Blain, K.; Brewer, S. M.; Gonzalez, P.; Johnston, H. M.; Akkaraju, G., Dialing in on pharmacological features for a therapeutic antioxidant small molecule. *Dalton Transactions* **2019,** *48* (33), 12430-12439.

7. Johnston, H. M.; Pota, K.; Barnett, M. M.; Kinsinger, O.; Braden, P.; Schwartz, T. M.; Hoffer, E.; Sadagopan, N.; Nguyen, N.; Yu, Y.; Gonzalez, P.; Tircsó, G.; Wu, H.; Akkaraju, G.; Chumley, M. J.; Green, K. N., Enhancement of the Antioxidant Activity and Neurotherapeutic Features through Pyridol Addition to Tetraazamacrocyclic Molecules. *Inorganic Chemistry* **2019,** *58* (24), 16771-16784.

8. Lincoln, K. M.; Gonzalez, P.; Richardson, T. E.; Julovich, D. A.; Saunders, R.; Simpkins, J. W.; Green, K. N., A potent antioxidant small molecule aimed at targeting metal-based oxidative stress in neurodegenerative disorders. *Chemical Communications* **2013,** *49* (26), 2712-2714.

9. Lincoln, K. M.; Richardson, T. E.; Rutter, L.; Gonzalez, P.; Simpkins, J. W.; Green, K. N., An N-Heterocyclic Amine Chelate Capable of Antioxidant Capacity and Amyloid Disaggregation. *ACS Chemical Neuroscience* **2012,** *3* (11), 919-927.

10. Lincoln, K. M.; Gonzalez, P.; Richardson, T. E.; Rutter, L.; Julovich, D. A.; Simpkins, J. W.; Green, K. N., A potent antioxidant small molecule aimed at targeting metal-based oxidative stress in neurodegenerative disorders. *Chem. Commun.* **2013,** *49*, 2712-2714.

11. Tutughamiarso, M.; Pisternick, T.; Egert, E., Pseudopolymorphs of chelidamic acid and its dimethyl ester. *Acta Crystallographica Section C* **2012,** *68* (9), o344-o350.

12. Alkorta, I.; Elguero, J., A density functional theoretical study of the influence of cavities and water molecules on tautomerism: The case of pyridones and 1,2,4-triazoles linked to crown ethers and esters. *Journal of Heterocyclic Chemistry* **2001,** *38* (6), 1387-1391.

13. Hall, A. K.; Harrowfield, J. M.; Skelton, B. W.; White, A. H., Chelidamic acid monohydrate: the proton complex of a multidentate ligand. *Acta Crystallographica Section C* **2000,** *56* (4), 448-450.

14. Aghabozorg, H.; Firoozi, N.; Roshan, L.; Eshtiagh-Hosseini, H.; Salimi, A. R.; Mirzaei, M.; Ghanbari, M.; Shamsipur, M.; Ghadermazid, M., Supramolecular structure of calcium(II) based on chelidamic acid: An agreement between theoretical and experimental studies. *Journal of the Iranian Chemical Society* **2011,** *8* (4), 992-1005.

15. Lincoln, K. M.; Offutt, M. E.; Hayden, T. D.; Saunders, R. E.; Green, K. N., Structural, Spectral, and Electrochemical Properties of Nickel(II), Copper(II), and Zinc(II) Complexes Containing 12-Membered Pyridine- and Pyridol-Based Tetra-aza Macrocycles. *Inorg. Chem.* **2014,** *53* (3), 1406-1416.

16. Chai, J.-D.; Head-Gordon, M., Long-range corrected hybrid density functionals with damped atom–atom dispersion corrections. *Physical Chemistry Chemical Physics* **2008,** *10* (44), 6615-6620.

17. Petersson, G. A.; Bennett, A.; Tensfeldt, T. G.; Al-Laham, M. A.; Shirley, W. A.; Mantzaris, J., A complete basis set model chemistry. I. The total energies of closed-shell atoms and hydrides of the first-row elements. *The Journal of Chemical Physics* **1988,** *89* (4), 2193-2218.

18. Marenich, A. V.; Cramer, C. J.; Truhlar, D. G., Universal Solvation Model Based on Solute Electron Density and on a Continuum Model of the Solvent Defined by the Bulk Dielectric Constant and Atomic Surface Tensions. *The Journal of Physical Chemistry B* **2009,** *113* (18), 6378-6396.

19. Tyl, A.; Nowak, M.; Kusz, J., Two polymorphs of anhydrous 4-pyridone at 100 K. *Acta Cryst.* **2008,** *C64*, 661-664.

20. Flakus, H. T.; Tyl, A., Electron-induced phase transition in hydrogen-bonded anhydrous solid state 4-pyridone. *Vibrational Spectroscopy* **2012,** *63*, 440-450.

21. Wójcik, G.; Mossakowska, I., Polymorphs of p-nitrophenol as studied by variable-temperature X-ray diffraction and calorimetry: comparison with m-nitrophenol. *Acta Cryst.* **2006,** *B62*, 143-152.

22. Maison, W.; Kennedy, R. J.; Kemp, D. S., Chaotropic Anions Strongly Stabilize Short, N-Capped Uncharged Peptide Helicies: A New Look at the Perchlorate Effect. *Angewandte Chemie International Edition* **2001,** *40* (20), 3819-3821.

23. Bruker-Nano *APEX3 : Suite for Crystallographic Software. Single Crystal*, V2019; Bruker Nano Inc: Madison WI, 2019.